Flexible joints control: a minimum-time feed-forward technique

Luca CONSOLINI, Oscar GERELLI, Corrado GUARINO LO BIANCO,
Aurelio PIAZZI

Dip. di Ing. dell'Informazione, University of Parma, I-43100 Parma, Italy
{`lucac,gerelli,guarino,piazzi`}`@ce.unipr.it`

Abstract

The paper proposes a linear programming approach to the feedforward minimum-time control of flexible joints. Taking into account both input and output constraints, the optimal bang-bang control is computed by discretizing a continuous-time joint model and by solving a sequence of linear programming feasibility problems. The resulting joint motion is a smooth rest-to-rest motion without oscillations. Theoretical analysis is presented and proof of convergence is given. Experimental results illustrate the proposed open-loop technique. Comparison with inversion based techniques is also discussed.

Key words: Minimum-time control, Flexible joints, Feed-forward control

---

1 Introduction

Time minimization is an important issue in robotics applications where production rates cover a relevant role. Unfortunately, any minimum time performance is usually achieved by maximizing the actuator dynamic efforts. This can lead, in the case of standard feedback controllers, to undesirable results, such as saturations with consequent output overshoots and oscillations. These effects are even more relevant in robotic applications showing a significant elastic coupling between joints. A typical application could be represented, for example, by robots sharing their workspace with human beings: the use of elastic joint increases the system safety by reducing the arm stiffness. For such kind of robots, any sudden torque change, an implicit requirement of minimum-time motions, can excite the oscillatory dynamics. It is therefore important to introduce, together with the usual input constraints considered in the robotic literature, also output constraints. In this paper a time-optimal solution for an electrically driven flexible joint arm is proposed. Explicit bounds on the motor feeding voltage are considered but, at the same time, a zero overshoot solution is required.

Preprint submitted to Elsevier *30 April 2007*

The minimum-time problem is solved by discretizing the continuous-time system and formulating an equivalent discrete-time optimization problem solved by means of linear programming techniques. Indeed, in the discrete-time case, input and output constraints can be written as linear inequalities and the minimum number of steps needed for a rest-to-rest transition can be found with a sequence of feasibility tests of an appropriate linear programming problem.

The use of linear programming techniques for solving minimum-time problems for linear discrete-time systems subject to bounded inputs dates back to Zadeh [9]. Subsequently, many contributions have appeared focusing on various improvements. For example a faster algorithm is proposed in [2]: it can compute the minimum-time optimal control in a single run. The work [5] presents a more general linear programming algorithm for solving optimal control problems for linear systems under general constraints. In [4] a feasibility test is presented to improve the algorithm speed. For what concerns time-optimal control for continuous time systems, a related result, under different hypotheses, is presented in [8]. It applies a comparison principle to a time-optimal control problem for a class of state-constrained second-order systems.

The paper is organized as follows. In §2 the dynamic model of a flexible joint is devised. It will be used for the synthesis and the validation of the proposed control technique. In §3 the control problem is proposed and a solution is obtained in the subsequent section by means of a linear programming algorithm. An experimental test case is discussed in §5, while §6 draws the final conclusions.

Notation: Given a sequence $u(k) : \mathbb{Z} \to \mathbb{R}$, $U(z) = \mathcal{Z}\{u(k)\}$ represents its Z-transform, $\|u(k)\|_\infty = \max\{|u(k)| : k \in \mathbb{Z}\}$ is the infinity norm of $u(k)$. For $x \in \mathbb{R}$, $\lfloor x \rfloor = \max\{i \in \mathbb{Z} | i < x\}$ is the floor of x and $1_n \in \mathbb{R}^n = (1, 1, \ldots, 1)^T$. Given a matrix $M \in \mathbb{R}^{n\times n}$, $\|M\|_2 = \max\{\|Ax\| : x \in \mathbb{R}^n \text{ with } \|x\| = 1\}$ is the 2-norm.

2 Flexible joint model

The flexible joint system considered in this paper is an educational mechatronic device designed by Quanser Consulting. Fig. 1 shows the top view of the experimental device: a rigid arm is connected, through a flexible joint, to a rotating "body", which is actuated by a servo motor. Both the body and the arm can rotate around vertical axis *"O"* of Fig. 1. The elastic coupling between the body and the arm is obtained by means of two springs whose stiffness is K_e and whose unstretched length is l_0.

The control technique proposed in §4 is based on the knowledge of the system model. For this reason, an accurate nonlinear model, mainly used for simulation purposes, is proposed in the following. The linearized version of the same model, to be used for the controller synthesis, is then devised.

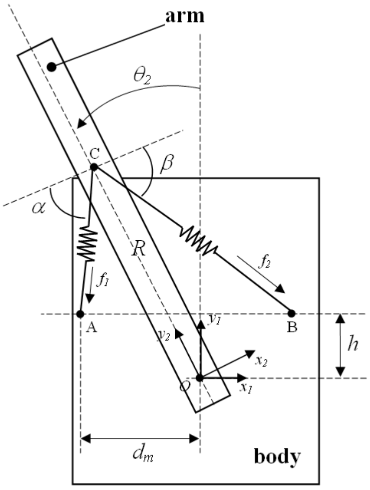

Fig. 1. Flexible joint experiment: Top view.

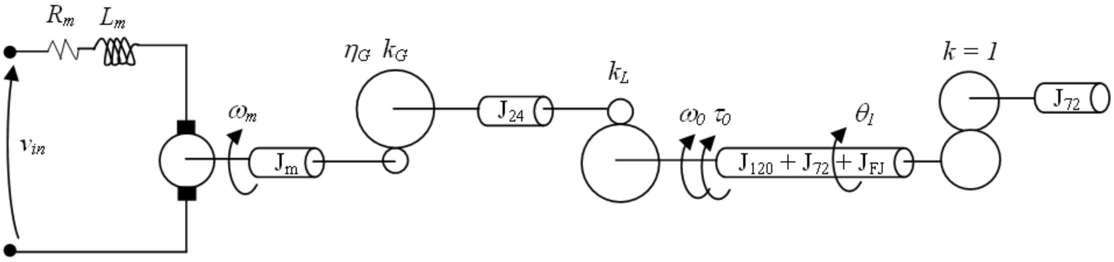

Fig. 2. Inertia and gearboxes ratio chain view from motor rotor axis

Spring forces $\mathbf{f}_1$ and $\mathbf{f}_2$ cover an important role in the system dynamics. In order to evaluate their amplitude, let us assign a reference frame $\{1\}$ whose origin is located in *"O"* and integral with the body. Moreover, let us assign a further frame $\{2\}$, located in *"O"* but integral with the arm, and indicate by θ_2 the joint angle between the two frames. Angle θ_2 is counterclockwise positive. In the same way, let us indicate by θ_1 the counterclockwise positive joint angle between the body frame $\{1\}$ and a given stationary frame.

The three points *"A"*, *"B"*, and *"C"* shown in Fig. 1 can be described with respect to frame $\{1\}$ by means of three vectors $\mathbf{p}_a := [-d_m \; h]^T$, $\mathbf{p}_b := [d_m \; h]^T$, and $\mathbf{p}_c := [-R\sin\theta_2 \; R\cos\theta_2]^T$ where d_m, h, and R are the geometrical dimensions reported in the same figure.

The spring force norms, i.e., $f_1 := \|\mathbf{f}_1\|$ and $f_2 := \|\mathbf{f}_2\|$, depend on the spring lengths l_1 and l_2 according to equations

$$f_1 = K_e(l_1 - l_0) \, , \tag{1}$$

$$f_2 = K_e(l_2 - l_0) \, , \tag{2}$$

where l_1 and l_2 can be evaluated as follows

$$
\begin{aligned}
l_1 &= \|\mathbf{p}_c - \mathbf{p}_a\| \\
&= \sqrt{R^2 + d_m^2 + h^2 - 2R(d_m \sin\theta_2 + h\cos\theta_2)}\ , \qquad (3) \\
l_2 &= \|\mathbf{p}_c - \mathbf{p}_b\| \\
&= \sqrt{R^2 + d_m^2 + h^2 + 2R(d_m \sin\theta_2 - h\cos\theta_2)}\ . \qquad (4)
\end{aligned}
$$

Forces acting on point *"C"* can be described with respect to frame $\{2\}$ leading to

$$
\begin{bmatrix} f_{1_x} \\ f_{1_y} \end{bmatrix} = \begin{bmatrix} f_1 \cos(\alpha) \\ f_1 \sin(\alpha) \end{bmatrix} = \begin{bmatrix} -K_e(l_1 - l_0)\cos(\alpha) \\ -K_e(l_1 - l_0)\sin(\alpha) \end{bmatrix}
$$

and

$$
\begin{bmatrix} f_{2_x} \\ f_{2_y} \end{bmatrix} = \begin{bmatrix} f_2 \cos(\beta) \\ f_2 \sin(\beta) \end{bmatrix} = \begin{bmatrix} K_e(l_2 - l_0)\cos(\beta) \\ -K_e(l_2 - l_0)\sin(\beta) \end{bmatrix}
$$

where $\alpha, \beta \in \mathbb{R}^+$ are the two auxiliary angles shown in Fig. 1 which can be evaluated by means of the following equations

$$
\begin{aligned}
\alpha(\theta_2) &= \arctan\left[\frac{R\cos(\theta_2) - h}{d_m - R\sin(\theta_2)}\right] - \theta_2\ , \\
\beta(\theta_2) &= \arctan\left[\frac{R\cos(\theta_2) - h}{d_m + R\sin(\theta_2)}\right] + \theta_2\ .
\end{aligned}
$$

Elastic forces induce an elastic nonlinear torque in the arm that can be expressed as

$$
\tau_e = [-f_{1_x}(\theta_2) - f_{2_x}(\theta_2)]\, R\ . \qquad (5)
$$

It is worth noting that components f_{1_y} an f_{2_y} do not generate any torque with respect to *"O"*.

It is now possible to propose the dynamic equation of the rigid arm described with respect to *"O"*

$$
J_{load}(\ddot{\theta}_2 + \ddot{\theta}_1) = [-f_{1_x}(\theta_2) - f_{2_x}(\theta_2)]\, R - B_{eq}^L \dot{\theta}_2 \qquad (6)
$$

where J_{load} is the arm inertia evaluated with respect to *"O"*, while B_{eq}^L is the friction coefficient associated to angular velocity $\dot{\theta}_2$. Practically, arm dynamics takes into account torques which are due to inertia, friction and elasticity.

Similarly, it is possible to devise the dynamic equation of the "body". It is made of an inertial load joined to an electric motor by means of a chain of reduction gears according to the scheme shown in Fig. 2. Even in this case, the system is affected by torques deriving from inertia, friction and elasticity

$$J_{eq}^{0}\ddot{\theta}_1 = \tau^0 - B_{eq}^{0}\dot{\theta}_1 - \left[-f_{1_x}(\theta_2) - f_{2_x}(\theta_2)\right] R + B_{eq}^{L}\dot{\theta}_2 \;, \tag{7}$$

where J_{eq}^{0} is the equivalent inertia of the system composed by motor, reduction gears, and "body", τ^0 is the motor torque, while B_{eq}^{0} is the friction coefficient associated to angular velocity $\dot{\theta}_1$. All the quantities in (7) are referred to the output shaft of the system. For a system like that shown in Fig. 2 the equivalent inertia can be expressed as

$$J_{eq}^{0} = \left[J_m k_g^2 k_l^2 \eta_g + J_{24} k_l^2 + J_{120} + 2J_{72} + J_{FJ}\right]$$

where k_g and k_l are gearbox reduction rates, J_{24}, J_{72}, and J_{120} are gearboxes inertias, J_{FJ} is the body inertia, J_m is the motor inertia, while η_g represents the efficiency of the motor gearbox.

Output torque τ_0 depends on the motor characteristics and on characteristics of the power train. It is possible to verify that it can be expressed as

$$\tau^0 = \frac{k_g k_l k_m \eta_g \eta_m}{R_m} v_{in} - \frac{k_g^2 k_l^2 k_m^2 \eta_g \eta_m}{R_m} \dot{\theta}_1 \tag{8}$$

where η_m is the motor efficiency, k_m is the motor electric constant, R_m is the motor winding resistance, and v_{in} is the motor feeding voltage.

Bearing in mind (8), it is possible to rewrite (7) as follows

$$J_{eq}^{0}\ddot{\theta}_1 = -G\dot{\theta}_1 + B_{eq}^{L}\dot{\theta}_2 - \left[-f_{1_x}(\theta_2) - f_{2_x}(\theta_2)\right] R + H v_{in} \;, \tag{9}$$

where

$$G = \frac{k_g^2 k_l^2 k_m^2 \eta_g \eta_m}{R_m} + \beta_{eq}^{0} \;, \tag{10}$$

$$H = \frac{k_g k_l k_m \eta_g \eta_m}{R_m} \;. \tag{11}$$

Equations (6) and (9) represent the complete nonlinear dynamic model of the flexible joint system and are used to simulate the system behaviour. For the synthesis of the control technique proposed in §4 an equivalent linear model is devised. Elastic torque τ_e is the sole nonlinear term which appears in (6) and (9). It can be linearized in $\theta_2 = 0$ leading to $\tau_e \simeq -K_{stiff}\theta_2$, where K_{stiff} is an equivalent stiffness constant. Consequently, (6) and (9) can be rewritten as

$$J_{eq}^{0}\ddot{\theta}_1 = -G\dot{\theta}_1 + B_{eq}^{L}\dot{\theta}_2 + K_{stiff}\theta_2 + H v_{in} \;, \tag{12}$$

$$J_{load}(\ddot{\theta}_2 + \ddot{\theta}_1) = -B_{eq}^{L}\dot{\theta}_2 - K_{stiff}\theta_2 \;. \tag{13}$$

Finally, it is possible to rewrite (12) and (13) into a state-space form $\dot{\mathbf{x}} = \mathbf{A}\mathbf{x} + \mathbf{b}\, v_{in}$ by assuming $\mathbf{x} := [x_1 x_2 x_3 x_4]^T = [\theta_1 \theta_2 \dot{\theta}_1 \dot{\theta}_2]^T$ and defining

$$\mathbf{A} := \begin{bmatrix} 0 & 0 & 1 & 0 \\ 0 & 0 & 0 & 1 \\ 0 & \frac{K_{stiff}}{J_{eq}^0} & -\frac{G}{J_{eq}^0} & \frac{B_{eq}^L}{J_{eq}^0} \\ 0 & -\frac{K_{stiff}(J_{load}+J_{eq}^0)}{J_{load}J_{eq}^0} & \frac{G}{J_{eq}^0} & -\frac{B_{eq}^L(J_{load}+J_{eq}^0)}{J_{load}J_{eq}^0} \end{bmatrix} \tag{14}$$

$$\mathbf{b} := \begin{bmatrix} 0 \\ 0 \\ \frac{H}{J_{eq}^0} \\ -\frac{H}{J_{eq}^0} \end{bmatrix} . \tag{15}$$

3 Problem formulation

In this section, the minimum-time feedforward control problem is stated for scalar discrete-time systems in a general case.

3.1 General formulation

A linear discrete-time system Σ_d is described by the proper scalar transfer function

$$H(z) = \frac{b(z)}{a(z)} = \frac{b_m z^m + b_{m-1} z^{m-1} + \cdots + b_0}{a_n z^n + a_{n-1} z^{n-1} + \cdots + a_0} \quad . \tag{16}$$

$a(z)$, $b(z)$ are coprime, Σ_d is stable, and its static gain $H(1) \neq 0$. The system input and output sequences are denoted by $u(k)$ and $y(k)$ respectively, $k \in \mathbb{Z}$.

The behavior $\mathcal{B}_d$ of system Σ_d is the set of all input-output pairs $(u(\cdot), y(\cdot))$, where $u(\cdot), y(\cdot) : \mathbb{Z} \to \mathbb{R}$, satisfying the difference equation:

$$\begin{aligned} & a_n y(k+n) + a_{n-1} y(k+n-1) + \cdots + a_0 y(k) = \\ & b_m u(k+m) + b_{m-1} u(k+m-1) + \cdots + b_0 u(k) . \end{aligned} \tag{17}$$

The set of input-output equilibrium points of Σ_d is $\mathcal{E} := \left\{ (u, y) \in \mathbb{R}^2 : y = H(1) u \right\}$ and the set $\mathcal{K}_s \subset \mathcal{B}_d$ of all rest-to-rest constrained transitions from $(0,0) \in \mathcal{E}$ to $(\frac{y_f}{H(1)}, y_f) \in \mathcal{E}$ is defined as follows.

Definition 1 *Given the parameter set* $\mathbf{s} := \{U_c, Y_c, y_f\}$ *where* $U_c = [u_c^-, u_c^+]$ *and* $Y_c = [y_c^-, y_c^+]$ *are the constraint intervals for the input and output respectively and* y_f *is the final rest value of the output,* $\mathcal{K}_\mathbf{s}$ *is the set of all pairs* $(u(\cdot), y(\cdot)) \in \mathcal{B}_d$ *for which there exists* $k_f \in \mathbb{N}$ *such that:*

$$u(k) = 0 \;\; \forall k < 0\,, \quad u(k) = \frac{y_f}{H(1)} \;\; \forall k \geq k_f\,, \tag{18}$$
$$u(k) \in U_c \;\; \forall k \in \mathbb{Z}\,, \tag{19}$$
$$y(k) = 0 \;\; \forall k < 0\,, \quad y(k) = y_f \;\; \forall k \geq k_f\,, \tag{20}$$
$$y(k) \in Y_c \;\; \forall k \in \mathbb{Z}\,. \tag{21}$$

The minimum-time feedforward constrained control problem for discrete-time systems consists in finding the optimal input sequence $u^*(k)$, $k = 0, 1, \ldots, k_f^* - 1$ for which the pair $(u^*(\cdot), y^*(\cdot)) \in \mathcal{K}_\mathbf{s}$ is a minimizer for the optimization problem:

$$k_f^* = \min_{(u(\cdot),y(\cdot)) \in \mathcal{K}_\mathbf{s}} K_f(u(\cdot), y(\cdot))\,. \tag{22}$$

$K_f(u(\cdot), y(\cdot))$, the rest-to-rest transition time associated to pair $(u(\cdot), y(\cdot))$, is defined as follows

$$K_f(u(\cdot), y(\cdot)) := \min\{k_1 \in \mathbb{N} : u(k) = \frac{y_f}{H(1)},\, y(k) = y_f\,, \forall k \geq k_1\}\,.$$

3.2 An approximated solution to the continuous time problem using discretization

Given a continuous system $H(s)$ a time-optimal constrained control problem can be converted to the discrete-time one defined above through the following procedure:

- find the discretized system $H(z)$ using a zero-order equivalence, with sampling period T, by applying relation $H(z) = (1 - z^{-1})\mathcal{Z}\{\frac{H(s)}{s}\}$;
- find the time-optimal input sequence $u^*(k)$;
- use for the continuous system the input function $u(t)$ obtained from the discrete sequence with a zero-order hold $u(t) = u^*(\lfloor \frac{t}{T} \rfloor)$, where $T \in \mathbb{R}$ is the sampling period.

3.3 Flexible-joint specific formulation

Consider the discrete system obtained by discretizing the rotary flexible joint system introduced in §2. Given two real intervals U_c, Y_c find the input sequence $u(k)$ that minimizes the time required for the rest-to-rest transition of the output $y(k)$

from the initial angle 0 to the final angle y_f, while satisfying the input and output constraints

$$u(k) \in U_c,\ y(k) \in Y_c,\ \forall k > 0\ .$$

4 Problem resolution

The key result upon which to build the solution to (22) is given by the next proposition.

Theorem 1 *Set $\mathcal{K}_s$ is not empty if*

$$\{0, \frac{y_f}{H(1)}\} \subset (u_c^-, u_c^+) \quad and \quad \{0, y_f\} \subset (Y_c^-, Y_c^+)\ . \tag{23}$$

The following lemma is used in the proof

Lemma 1 *Consider system (16), let it be $(u(k), y(k)) \in \mathcal{B}_d$. If*

$$\begin{aligned} y(i+N) &= y_f \text{ for } i = 0, \dots, n-1 \\ u(i+N) &= \tfrac{y_f}{H(1)} \text{ for } i \geq 0\ , \end{aligned}$$

then

$$y(i) = y_f, \forall i \geq N. \tag{24}$$

Proof of the lemma Consider the input-output couple $(u_2(k), y_2(k)) = (u(k) - \frac{y_f}{H(0)}, y(k) - y_f)$, it is $u_2(k) = 0$, $\forall k \geq N$, therefore, for $k \geq N$, $y_2(k)$ satisfies the following difference equation

$$\begin{cases} a_n y_2(k+n) = -a_{n-1} y(k+n-1) - a_{n-2} y_2(k+n-2) - \cdots - a_0 y_2(k) \\ y_2(N) = y_2(N+1) = \cdots = y_2(N+n-1) = 0\ , \end{cases}$$

which has the solution $y_2(k) = 0$, $\forall k \geq N$, from which (24) follows. $\square$

Proof of the theorem

Define a continuous function $l(t)$ with the following properties:

$$\begin{cases} l(t) = 0 \ \text{ if } \ t \leq 0 \\ l(t) = \frac{y_f}{H(1)} \ \text{ if } \ t \geq 1 \\ 0 \leq l(t) \leq \frac{y_f}{H(1)} \ \ \forall t \in [0,1] \end{cases}$$

Set $u_N(k) = l(\frac{k}{N})$ and let $U_N(z)$ be the corresponding Z-transform, let $Y_N(z) = U_N(z)H(z)$ and $y_N(k) = \mathcal{Z}^{-1}\{Y_N(z)\}$.

First of all we prove that

$$\lim_{N\to+\infty} ||H(1)\, u_N(k) - y_N(k)||_\infty = 0 \tag{25}$$

in fact

$$H(1)\, U_N(z) - Y_N(z) = H(1)\, U_N(z) - H(z)\, U_N(z) = (H(1) - H(z))\, U_N(z)\ ,$$

being $H(1) - H(z)|_{z=1} = 0$, function $H(1) - H(z)$ has a zero in $z = 1$ and $H(1) - H(z) = (z-1)H'(z)$, where $H'(z)$ has the same poles as $H(z)$. Therefore $(H(1) - H(z))\, U_N(z) = H'(z)(z-1)U_N(z)$ and

$$\lim_{N\to+\infty} ||H(1)\, u_N(k) - y_N(k)||_\infty \leq \lim_{N\to\infty} ||\mathcal{Z}^{-1}\{H'(z)\}||_2\ \ ||u_N(k+1) - u(k)||_\infty = 0\ ,$$

in fact

$$\lim_{N\to+\infty} ||u_N(k+1) - u(k)||_\infty = 0$$

because function $l(t)$ is uniformly continuous and $||\mathcal{Z}^{-1}\{H'(z)\}||_2$ is finite because $H'(z)$ is stable.

Equation (25) shows that as N approaches infinity, the output $y_N(k)$ becomes a copy of input $u_N(k)$ multiplied by the static gain $H(1)$ and, for $k \geq N$, the difference $y_N(k) - y_f$ tends to zero. In the following we define a correcting term $\bar{y}_N(k)$ such that $y_N(k) + \bar{y}_N(k) = y_f$, $\forall k \geq N$ exactly. Define the error function $e_N \in \mathbb{R}^n$ as

$$e_N(i) = y_N(N+i) - y_f,\ \ i = 0, \dots, n-1\ ,$$

let $M \in \mathbb{R}^{n\times M}$ be such that

$$M_{ij} = h(j-i),\ \ i = 1, \dots, n,\ \text{ and }\ j = 1, \dots, N\ ,$$

where $h(k) = \mathcal{Z}^{-1}\{H(z)\}$ denotes the system impulse response. Define the correcting input function

$$\begin{cases} \bar{u}_N(k) = -M^+ e_N,\ \text{if } 0 \leq k < N\ , \\ 0 \text{ otherwise} \end{cases}$$

where $M^+ = M^t(M^tM)^{-1}e_N$ is the pseudo-inverse of M and let $\bar{y}_N(k)$ be the corresponding output. Consider as input $u_N(k)+\bar{u}_N(k)$, the corresponding output is $y_N(k)+\bar{y}_n(k)$. The following conditions are satisfied:

$$y_N(k)+\bar{y}_N(k)=y_f,\ \forall k \geq N\ , \tag{26}$$

$$\lim_{N\to+\infty} \|\bar{u}_N(k)\|_\infty = 0, \tag{27}$$

$$\lim_{N\to+\infty} \|\bar{y}_N(k)\|_\infty = 0. \tag{28}$$

If fact (26) follows from the fact that

$$y_N(N+k)+\bar{y}(N+k) = y_f + e_N(k) - e_N(k) = y_f.\ k=0,\ldots,n-1\ ,$$

and $y_N(k)+\bar{y}_N(k) = y_f$, $\forall k \geq N$ as a consequence of Lemma 1. Conditions (27) and (28) follows from

$$\lim_{N\to+\infty} \|\bar{u}_N(k)\|_\infty \leq \|M^+\|_2 \lim_{N\to+\infty} \|e_n\|_\infty = 0\ ,$$
$$\lim_{N\to+\infty} \|\bar{y}_N(k)\|_\infty \leq \|h(k)\|_2\|M^+\|_2 \lim_{N\to+\infty} \|e_n\|_\infty = 0\ ,$$

being $\lim_{N\to\infty} \|e_n\|_\infty = 0$ by (25).

Therefore

$$\begin{aligned}\lim_{N\to\infty} \max\Big\{ & u_N(k)+\bar{u}_N(k) - \frac{y_f}{H(1)}, -u_N(k)-\bar{u}_N(k), \\ & y_N(k)+\bar{y}_N(k)-y_f, -y_N(k)-\bar{y}_N(k)\Big\} = 0\end{aligned}$$

and, because of (23), for N sufficiently large the following property holds

$$\begin{aligned}\max\big\{ & u_N(k)+\bar{u}_N(k)-u_c^+, -u_N(k)-\bar{u}_N(k)-u_c^-, \\ & y_N(k)+\bar{y}_N(k)-y_c^+, -y_N(k)-\bar{y}_N(k)-y_c^-\big\} < 0\ ,\end{aligned} \tag{29}$$

therefore all properties (18)-(21) are verified. In fact (18) is verified by construction, (20) comes from (26) and (19), (21) follow from (29). □.

The following proposition allows to restate the time optimal problem in the form of linear programming.

Proposition 1 *The set $\mathcal{K}_s$ of all rest-to-rest constrained transitions is not empty if and only if there exist $k_f \in \mathbb{N}$ and a vector $\mathbf{u} \in \mathbb{R}^{k_f}$ for which the following LP problem is feasible:*

$$y_c^- \cdot \mathbf{1}_{k_f} \leq \mathbf{Hu} \leq y_c^+ \cdot \mathbf{1}_{k_f} \tag{30}$$

$$u_c^- \cdot \mathbf{1}_{k_f} \leq \mathbf{u} \leq u_c^+ \cdot \mathbf{1}_{k_f} \tag{31}$$

$$\bar{\mathbf{H}} \left[\begin{array}{c} \mathbf{u} \\ \hline \dfrac{y_f}{H(1)} \cdot \mathbf{1}_n \end{array}\right] = y_f \cdot \mathbf{1}_n \tag{32}$$

where $\mathbf{H} \in \mathbb{R}^{k_f \times k_f}$ *is defined by* $\mathbf{H}_{ij} := h(i-j)$ *and* $\bar{\mathbf{H}} \in \mathbb{R}^{n \times (k_f+n)}$ *by* $\bar{\mathbf{H}}_{ij} := h(i+k_f-j)$*.*

Proof.(Necessity) Assume that there exists a vector $\mathbf{u}$ for which equations (30)–(32) are satisfied. Define the input sequence

$$u(k) = \begin{cases} 0 \text{ if } k < 0 \\ \mathbf{u}(k) \text{ if } 0 \leq k < k_f \\ \frac{y_f}{H(1)} \text{ if } k \geq k_f \ , \end{cases} \tag{33}$$

which satisfies Properties (18) and (19) of Definition 1. The output is given by $y(k) = \sum_{i=0}^{\infty} u(k-i)h(i)$, where $h(k)$ is the impulse response of the discrete system. Setting $\mathbf{y} \in \mathbb{R}^{k_f} : \mathbf{y}(i) = y(i)$ and $\bar{\mathbf{y}} \in \mathbb{R}^n : \bar{\mathbf{y}}(i) = y(k_f+i)$, it is

$$\mathbf{y} = \mathbf{H}\mathbf{u} \ , \ \bar{\mathbf{y}} = \bar{\mathbf{H}} \left[\begin{array}{c} \mathbf{u} \\ \hline \dfrac{y_f}{H(1)} \cdot \mathbf{1}_n \end{array}\right] \ ,$$

and, by (30), $y(k)$ satisfies Property (21) of Definition 1, $\forall k < k_f$. Finally $y(k) = y_f$, $\forall k \geq k_f$ because of Lemma 1.
(Sufficiency) Assume that for a given k_f, the set $\mathcal{K}_s$ is non empty, therefore it contains a couple $(u(k), y(k))$. If $\mathbf{u}$ and $\mathbf{y}$ are defined as above, by properties (19) and (21) it follows that

$$u_c^- \cdot \mathbf{1}_{k_f} < \bar{u} < u_c^+ \cdot \mathbf{1}_{k_f}$$
$$y_c^- \cdot \mathbf{1}_{k_f} < \bar{y} < y_c^+ \cdot \mathbf{1}_{k_f} \ ,$$

moreover, being $y(k) = \sum_{i=0}^{+\infty} h(k-i)u(i)$,

$$\left[\begin{array}{c} \mathbf{y} \\ \hline \bar{\mathbf{y}} \end{array}\right] = \left[\begin{array}{c} \mathbf{H}|0 \\ \hline \bar{\mathbf{H}} \end{array}\right] = \left[\begin{array}{c} \bar{u} \\ \hline \dfrac{y_f}{H(1)} \cdot \mathbf{1}_n \end{array}\right] \ ,$$

therefore equations (30)–(32) are satisfied. □

By virtue of Proposition 1, the minimum-time k_f^* and an associated optimal feedforward input $u^*(k)$, $k = 0, 1, \ldots k_f^* - 1$ can be determined by means of a sequence of LP feasibility tests (the problem defined at (30)-(32)) through a simple bisection algorithm reported below. In this algorithm $LPP(\mathbf{s}, k_f, \mathbf{u})$ denotes a linear programming procedure that solves problem (30)-(32): if the problem is feasible it returns a Boolean true value along with a solution $\mathbf{u}$.

Algorithm: MTC

Compute the minimum-time feedforward control with input and output constraints for discrete-time systems

```
input  : $H(z)$ and $\mathbf{s}$
output: $k_f^*$ and $u^*(k)$, $k = 0, 1, \ldots, k_f^* - 1$
begin
    $k_f \longleftarrow 1$;
    $l \longleftarrow 0$;
    while $\sim LPP(\mathbf{s}, k_f, \mathbf{u})$ do
        $l \longleftarrow k_f$;
        $k_f \longleftarrow 2k_f$
    $h \longleftarrow k_f$;
    while $h - l > 1$ do
        $k_f \longleftarrow \lfloor \frac{h+l}{2} \rfloor$;
        if $\sim LPP(\mathbf{s}, k_f, \mathbf{u})$ then
            $l \longleftarrow k_f$;
        else
            $h \longleftarrow k_f$
    $k_f^* \longleftarrow h$;
    $u^*(k) \longleftarrow \mathbf{u}$
end
```

Remark 1 *Differently from the continuous case, the discrete minimum-time solution $u^*(k)$ is not unique (see[1]).*

5 Simulation and experimental results

Simulation are executed on a P4 3.0Ghz computer within Matlab programming environment. The freely available library QSopt is used as linear programming solver. Experimental results are obtained by interfacing the flexible joint device to Matlab through the Quanser Q4 PCI data acquisition board governed by WinCon real-time software.

By substituting the flexible joint parameters in state-space model, described in (14) and (15), the following numerical representation for the plant is achieved

$$\mathbf{A} := \begin{bmatrix} 0 & 0 & 1 & 0 \\ 0 & 0 & 0 & 1 \\ 0 & 379.9 & -56.65 & 2.956 \\ 0 & -512.9 & 56.65 & -3.99 \end{bmatrix}$$

$$\mathbf{b} := \begin{bmatrix} 0 \\ 0 \\ 93.74 \\ -93.74 \end{bmatrix} \tag{34}$$

5.1 Control without constraint on joint solicitation torque

The time-optimal feedforward control $u^*(t)$ has been obtained with the algorithm described in §4, to get a rest-to-rest transition from $y = 0$ to $y = \pi/4 (= y_f)$. Since the maximum bidirectional output voltage of the amplifier used to control the flexible joint is equal to 5 *Volts*, the input constraint is given by $\|u(t)\|_\infty \leq 5$, so that $U_c = [-5, +5]$. A strong requirement has been set on the output function: a maximum of 0.1% overshoot and undershoot on y is allowed, so that $Y_c = [-7.8539e-4, \pi/4 \ + 7.8539e-4]$.

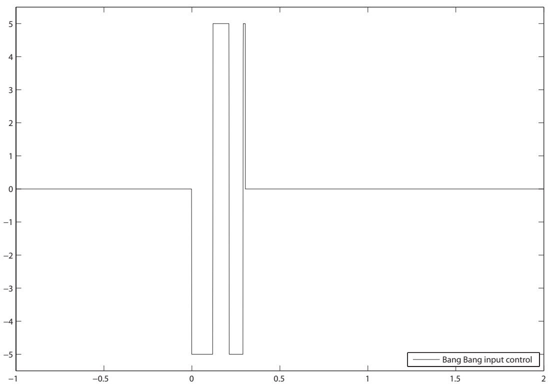

Fig. 3. Optimal reference input signal

The simulation sampling time is given by $T_s = 0.001$ s and the results are presented in Figures 3 and 4.

Figure 3 shows the bang-bang control input that allows to obtain a rest-to-rest transition time of $t_f^* = 0.31$ s. Figure 4 plots a comparison between the ideal simulated output signal and the real behaviour of the flexible joint. The real output shows a

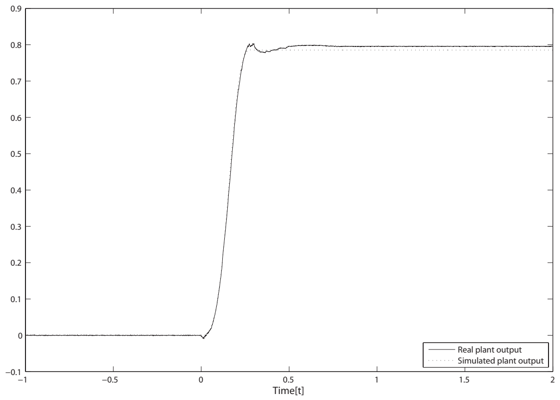

Fig. 4. Expected system output y (dashed line) and measured plant output (solid line)

$\Delta\theta$ (rad)	$T_s(s)$	Execution Time (s)
$\pi/4$	0.001	4.229
	0.010	0.5
	0.050	0.437
$\pi/2$	0.001	5.213
	0.010	0.6
	0.050	0.453

Table 1
Algorithm Perfomances

small overshoot and undershoot: this is due to the small mismatch existing between the real plant and the flexible joint model devised in §2 where all the nonlinearities of the mechatronic device are linearized.

In table 1 are shown the computation time needed by the proposed approach in order to devise the time-optimal control sequence. The symbol $\Delta\theta$ has been used for the overall rest-to-rest transition required for the system, while T_s indicate the sample time used in the discretization phase. As you can see performances are poorly related to the amplitude of the transition and they strongly depend on the sampling time used in the discretization phase: the higher is the sampling time the shorter is the computation time. Generally the time needed by the algorithm to obtain the time-optimal control is in the order of magnitude of a few seconds. Thus the proposed approach can be used in a real-time context since performances are predictable once the sampling time is set and, moreover, they can be improved if the algorithm is coded directly in C/C++.

The previously described approach has been compared with the one presented in [7] and [3], where a specific type of time-optimal control is found by means of dynamic inversion from inputs built on “transition polynomials” (see [7] for details).

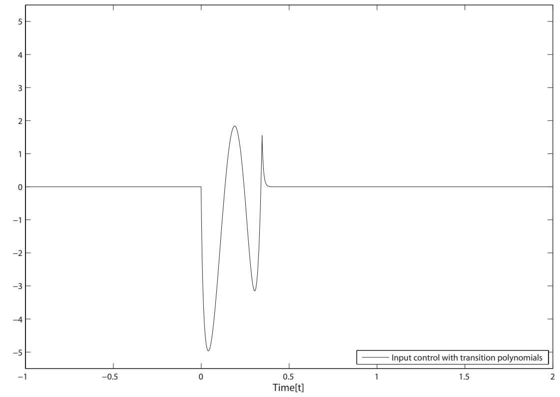

Fig. 5. Optimal transition polynomial input signal

For brevity we recall here only the general expression of this type of interpolating polynomials that allows an arbitrarily smooth transition between two constant output values (in this case 0 and $\pi/4$):

$$y(t;\tau) = \begin{cases} 0 \quad \text{if} \quad t \leq 0, \\ \frac{(2k+1)!}{k!\tau^{2k+1}} \sum_{i=0}^{k} \frac{(-1)^{k-i}}{i!(k-i)!(2k-i+1)} \tau^i t^{2k-i+1} \quad \text{if} \quad 0 \leq t \leq \tau, \\ \pi/4 \quad \text{if} \quad t \geq \tau \end{cases}$$

where y is the desired output function, k is the relative order of the plant transfer function and τ is the minimum transition time. In this case the plant transfer function, from (34), is equal to:

$$H(s) = \frac{-96.97s - 1.247 \cdot 10^4}{s^4 + 60.64s^3 + 571.5s^2 + 7534s}$$

thus the relative order is $k = 3$.

Results obtained with this last technique are presented in Figures 5 and 6. The time optimal rest-to-rest transition is performed in $t_f^* = 0.36$ s. The minimum-time approach based on “transition polynomials” allows to generate a smoother input control at a price of a longer task activity time, even for a small transition angle as the one showed here.

5.2 Control with constraint on joint solicitation torque

The minimum-time control law used in the previous simulations and experiments does not take care of the solicitation torque induced to the joint by the deflection

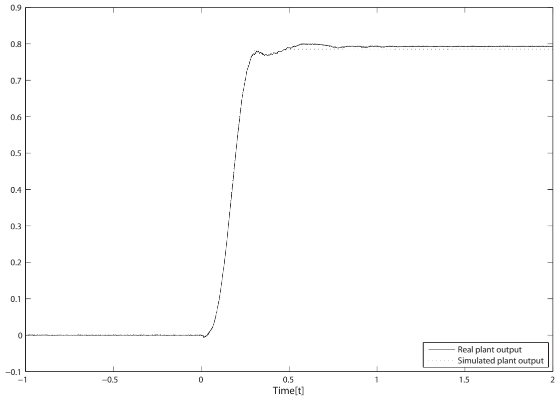

Fig. 6. Expected system output y (dashed line) and measured plant output (solid line)

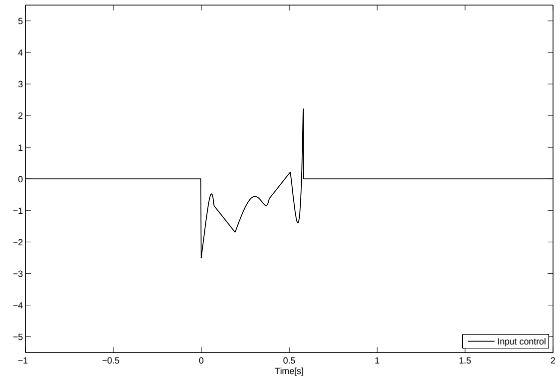

Fig. 7. The time-optimal control with angle limit on θ_2

angle θ_2: the only constraint that has been imposed is related to the end-effector position, i.e. the sum of $\theta_1 + \theta_2$.

On a real flexible-joint robot one can be interested in determining a time-optimal transition control in which the maximum admissible displacement between the link position and the joint position is constrained, thus reducing the mechanical solicitation on the joint itself.

The proposed approach has been described in detail for the SISO (Single Input - Single Output) case, but its extension to the multi variable case is straightforward since all the previous theoretical considerations are valid.

Then, under the same constraints used in previous section, a limit on θ_2 angle has been added such that $\theta_2 \in [-5\pi/180, 5\pi/180]$.

Simulated and experimental results are reported in figure 7 and 8. In particular in figure 9 is reported the time-waveform of the relative displacement between the arm and the rotating body. As it is shown, the θ_2 angle is constantly keeps saturated to the imposed constraint value, and this is the reason why the optimal control is no longer a bang-bang function.

Clearly the optimal transition time increases to $t_f^* = 0.59$ s.

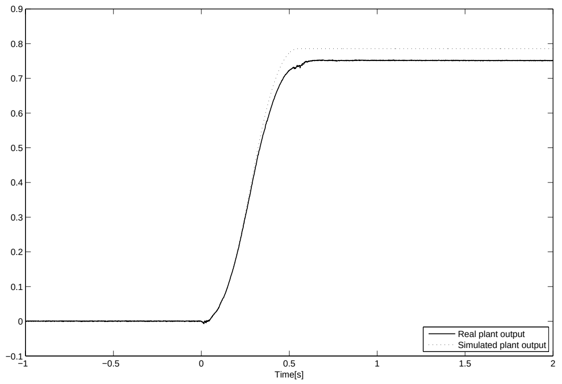

Fig. 8. Expected system output y (dashed line) and measured plant output (solid line)

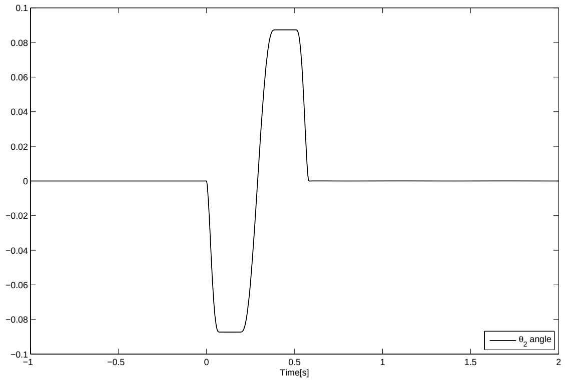

Fig. 9. θ_2 angle

6 Conclusions

The paper has proposed a linear programming algorithm to compute the globally optimal minimum-time control for rest-to-rest constrained transitions of flexible joints. A comparison with the alternative inversion-based feedforward control has confirmed the effectiveness of the new approach. Moreover this approach applies to any stable linear plant so that it is foreseeable the extension of the technique to the more challenging cases of systems with unstable zero-dynamics such as, for example, flexible links [6].

References

[1] Desoer C. A. and Wing J. A minimal time discrete system. *IRE Transactions on Automatic Control*, 1961.

[2] Bashein G. A simplex algorithm for on-line computation of time optimal controls. *IEEE Transactions on Automatic Control*, 1971.

[3] C. Guarino Lo Bianco and A. Piazzi. A servo control system design using dynamic inversion. *Control Engineering Practice*, 10(8):847–855, August 2002.

[4] M. H. Kim and S. Engell. Speed-up of linear programming for time-optimal control. *Proc. of the 1994 American Control Conference, ACC94*, pages 2667–2670, 1994.

[5] Scott M. Time/fuel optimal control of constrained linear discrete systems. *Automatica*, 1986.

[6] A. Piazzi and A. Visioli. End-point control of flexible link via optimal dynamic inversion. In *Proceedings of the 2001 IEEE/ASME International Conference on Advanced Intelligent Mechatronics*, pages 936–941, Como, Italy, July 2001.

[7] A. Piazzi and A. Visioli. Optimal noncausal set-point regulation of scalar systems. *Automatica*, 37(1):121–127, January 2001.

[8] Kim S., Choi D., and Ha I. A comparison principle for state-constrained differential inequalities and its application to time-optimal control. *Automatic Control, IEEE Transactions on*, 2005.

[9] L. A. Zadeh. On optimal control and linear programming. *IRE Transactions on Automatic Control*, pages 45–46, 1962.